Volume 9, Issue 6, 2019, 4605 - 4611 ISSN 2069-5837

Biointerface Research in Applied Chemistry

www.BiointerfaceResearch.com

https://doi.org/10.33263/BRIAC96.605611

Original Research Article Open Access Journal

Received: 30.09.2019 / Revised: 12.11.2019 / Accepted: 14.11.2019 / Published on-line: 20.11.2019

Formation of microspherical particles of albumin with model drug using spray drying process

Artur Boldyrev [1], Marat Ziganshin [1,*], Timur Mukhametzyanov [1], Alexander Klimovitskii [1], Nikolay Lyadov [2,3], Alexander Gerasimov [1,*]

[1]1Department of Physical Chemistry, A.M. Butlerov Institute of Chemistry, Kazan Federal University, Kremlevskaya, 18, Kazan, 420008, Russia
[2]ZPTI-Subdivision, FIC KazanSC of RAS, Sibirsky Trakt 10/7, Kazan, 420029, Russia
[3]Institute of Engineering, Kazan Federal University, Kremlevskaya, 18, Kazan, 420008, Russia
*corresponding author e-mail address: ***alexander.gerasimov@kpfu.ru*** | Scopus ID 40661183600

ABSTRACT

Spray drying method enables to produce microspherical particles with narrow size distribution. Production of such microparticles is relevant for the development of the advanced systems for inhalation delivery of drugs. The aerosol particles diameter must be between 1 and 3 μm. Composite microparticles based on bovine serum albumin and model drug phenacetin were produced in the present work using the spray-drying method. The absence of a crystalline phase of the drug in composite microparticles was verified using several physicochemical methods. The average radius of the produced microparticles was found to be 1 μm based on the results from scanning electron microscopy. The rate of the dissolution of the drug included in microparticles is faster than that of crystalline phenacetin. The obtained results can be used for the development of the method for preparation of composite microparticles based on protein molecules using the spray-drying technique.

Keywords: *bovine serum albumin; phenacetin; spray drying; microparticles; inhalation; dissolution.*

1. INTRODUCTION

Development of the drug-containing microspherical particles with narrow size-distribution is one of the key problems of the modern pharmaceutics. Such particles can be used for inhalation delivery providing non-invasive transport of the drug immediately to the arterial bloodstream, reducing the time needed to reach the working concentration of the drugs of both topical and systemic actions, while at the same time avoiding degradation of drugs in the liver common for the oral administration [1].

The applicability of the particles for inhalation delivery is determined by its size, which must be between 1 and 3 μm. Smaller particles are mostly exhaled from the lungs with the air, while bigger particles deposit in the upper respiratory tract [2]. The shape of the particles also plays an important role. Spherical particles have more favorable aerodynamic properties, compared to the irregularly shaped particles. Thus the former provides more uniform administration of the drug [3].

The main methods for the production of microparticles currently include spray-drying, solvent evaporation, emulsification, and others [4–6]. Spray-drying is a method with the most potential, which allows producing the particles with the desired size distribution in a controllable manner [7–9]. Changing of the conditions during spray-drying provides control both on the particle size and shape, and at the same time provides low residual solvent content in the particle [10].

In the development of the inhalation delivery systems, the rapid dissolution of the API must be ensured, as slow dissolution poses a risk of atelectasis [11]. Keeping in mind, that most of the modern active pharmaceutical ingredients have low solubility in water [12], use of matrix components providing rapid dissolution of the API is an obvious solution.

Synthetic polymers [13], polymers from the biological sources [14], and proteins that are biodegradable, biocompatible, and have low toxicity [15], can be used as matrixes for the composite microparticles.

Albumin, a most abundant protein of the blood plasma, is a promising protein component for the composite microparticles. It plays different roles in the blood, including maintaining osmotic pressure, neutralizing free radical, and passive transport [16]. It is a solubilizing agent in vivo, enhancing the solubility of the wide spectrum of biomolecules and drugs [17]. The ability of albumin for enhancing the bioavailability of the drugs results from its capability for the formation of complexes with APIs, through the two main binding centers [18]. Formation of complexes between bovine serum albumin (BSA) and the drugs increases the concentration of drugs with low solubility in the blood [19].

Albumin can be absorbed by epithelium of lungs, faster than expected absorption rates, based on its molecular weight [20] Moreover, BSA has secondary binding centers, further increasing the number of bonded molecules [21].

BSA was used as a carrier for the inclusion compound of progesterone in cyclodextrin. The increase in the rate of dissolution of the drug was demonstrated [22]. The effectiveness of BSA as a drug carrier was also shown earlier [23,24]. The use of BSA allows reducing cytotoxicity of the drug by a factor of 9 [25]. BSA can also be used as a theranostic agent [26]. Resveratrol was amorphized with using of BSA [27].

There are several works devoted to the preparation of the composite particles for the inhalation delivery in the literature, but the problem of compatibility between a particular drug and a protein matrix is still important. In the present work, the

composite microspherical particles of phenacetin and albumin were produced using a spray-drying method. Composite particles were investigated with a range of physicochemical methods. The enhancement of the dissolution rate of the model hydrophobic drug phenacetin included in the composite microparticles was determined.

2. MATERIALS AND METHODS

2.1. Materials.

Phenacetin 98% (PHE) (Aldrich, Lot #BCBD7322V) and bovine serum albumin (BSA) (Fisher Sci., Lot 62-1397) were used without further purification. Bidistilled water and absolute ethanol were used as solvents.

2.2. Simultaneous thermogravimetry and differential scanning calorimetry (TG/DSC).

Simultaneous thermogravimetry and differential scanning calorimetry (TG/DSC) analysis of initial samples, microparticles and physical mixture were performed using the STA 449F1 Jupiter (Netzsch, Germany) thermoanalyzer instrument in the range of temperatures from 40 to 160 °C (40 to 500 °C for initial samples) under dynamic atmosphere of argon with a flow rate of 75 ml/min [28]. In each experiment, the heating rate was 5 °C/min.

2.3. Differential scanning calorimetry (DSC).

The thermophysical parameters of PHE and BSA, as well as those of their mechanical mixtures and microparticles (i.e., enthalpies and temperatures of thermal effects) in the temperature range of 20 to 160 °C, were determined using DSC 204 F1 Phoenix (Netzsch, Germany) differential scanning calorimeter, as described earlier [29,30]. The sample masses were between 7.7 and 10.7 mg, the heating rate of 5 °C/min (cooling 10 °C/min) was used in all scans, the instrument was flushed with argon (150 ml/min).

2.4. Powder X-ray diffraction.

Powder X-ray diffraction (PXRD) studies of protein, PHE, their physical mixture, and composites were performed using a table-top diffractometer MiniFlex 600 (Rigaku, Japan) with a D/teX Ultra detector. In all measurements Cu Kα radiation (40 kV, 15 mA) was used, diffractograms were collected in the range of 2θ from 3 to 50° with 0.02° steps and 0.24 s exposure time at each point without sample rotation at room temperature [28,31].

2.5. Fourier transformation-infrared spectroscopy (FTIR) analysis of solid samples.

FTIR spectra of solid samples of pure BSA, PHE, their physical mixture, and composites were acquired in the 600-4000 cm^{-1} range. Data were collected using a FTIR spectrometer Vertex 70 (Bruker, Germany) with a germanium crystal single reflection ATR accessory (MIRacle, PIKE Technologies, USA). To remove atmospheric water vapor the instrument and sample chamber were purged with dry air. For each measurement 128 scans at a resolution of 2 cm^{-1} were gathered. Background spectra of the same resolution were subtracted from sample spectra.

2.6. Spray-drying.

BSA/PHE solution (1.6% w/v) was produced by dissolving 0.4 g of bovine serum albumin powder together with 0.08 g of PHE in 30 ml of water. The resulting solution was filtered with 0.22 μm pore size filters. Microparticles were created by Nano Spray dryer B90 (Buchi, Switzerland) in the open mode with 7.0 μm hole size spray caps, using 7 ml/min flow rate, drying air flow 130 l/min, and inlet temperature 95 °C. The collected powders were stored at room temperature (RT) in the Eppendorf tubes [32].

2.7. Drug contents in microparticles.

To assay the total drug content in the spray-dried particles they were dissolved in ethanol as described in [33] at 10 mg/ml concentration of microparticles. Before measurements, the mixture was left to equilibrate overnight at continuous stirring at RT. The resulting solutions were analyzed with Cary 100 UV-Vis Spectrophotometer (Agilent Technologies, Germany) at 245 nm with suitable dilutions. The drug concentration in the solution was calculated using a regression equation derived from the measured calibration curve.

2.8. Scanning electron microscopy.

The morphology of the microparticles was studied using Zeiss EVO 50 XVP scanning electron microscope (Carl Zeiss, Germany) in variable pressure mode, which is suitable for nonconducting and gas-emitting samples. The working chamber pressure was 20 to 30 Pa. Tetrasolid-state BSE reflected electron detector was used for imaging at an acceleration voltage of 20.0 kV. Distribution curves were produced with Image-Pro Plus 6.0.0.260 and Origin 8.1 software packages.

2.9. In vitro dissolution of phenacetin.

The kinetics of PHE dissolution from composites was examined with Dissotest CE1 (Sotax, Switzerland) (USP IV) in a closed-loop mode [34] on samples containing an equivalent amount of PHE (12.5 mg). The tests were performed at 37.0 °C with 17 ml/min flow rate, using phosphate buffer with pH 6.86 as a dissolution medium. Solution was sampled at different times (at 1, 2, 3, 4, 5, 10, 15, 20, 25, 30, 60, 90, 120, 150, 180 minutes elapsed time) for analysis. Taken volume was replenished with the same amount (4ml) of fresh medium. PHE content was measured spectrophotometrically at 245 nm with Cary 100 UV-Vis Spectrophotometer (Agilent Technologies, Germany) with suitable dilutions.

2.10. Molecular docking.

Molecular docking studies were carried out using Autodock 4.2 and Autodock tools (ADT) using a Lamarckian genetic algorithm [35]. The crystallographic structure of BSA (PDB id: 3V03) and 3D structure of phenacetin (CID 4754) were taken from Brookhaven Protein Data Bank and DrugBank respectively. The optimization of parameters was performed according to the algorithm described in [36]. Simulations were performed for two BSA domains separately. Cell sizes were set to 126×98×126, axes lengths 0.719 Å and 126×88×126, axes lengths 0.681 Å for domains A and B respectively. Results of docking were visualized with the Autodock tools software package

2.11. Statistical analysis.

Statistical analyses were performed using Student's t-test or one-way analysis of variance (ANOVA). A p-value of < 0.05 was deemed significant in all cases. The uncertainties are expressed as a mean standard deviation from at least three independent experiments.

3. RESULTS

3.1. TG/DSC analysis of the initial compounds.

No significant weight loss is registered for PHE in the temperature range between 40 and 160 °C (Fig. 1). The thermal decomposition of PHE starts at temperatures above 180 °C. Thus all consequent DSC measurements of the composites containing PHE were performed at temperatures no higher than 160 °C. Endotherm with onset at 135.5 °C and enthalpy of 213.8 J/g, corresponding to the melting of PHE is clearly visible on the DSC scan (Fig. 1). The observed effects on the DSC curve at the temperature above 180 °C are related to the thermal degradation of PHE.

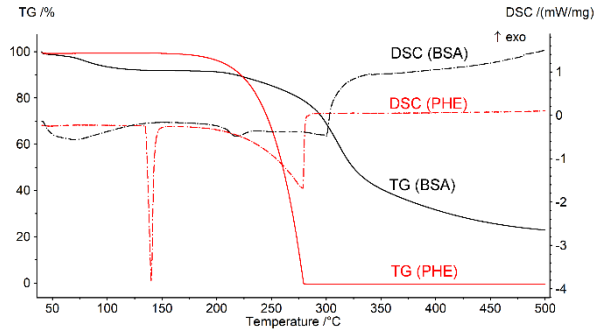

Figure 1. TG/DSC analysis of PHE and BSA in the temperature range from 40 to 500 °C in the dynamic argon atmosphere (75 ml/min).

A mass loss (8.16 %), related to the loss of water, is evident in the BSA scan in the temperature range between 40 and 150 °C. Decomposition of BSA proceeds at temperatures above 200 °C.
High thermal stability of BSA and PHE permits spray-drying at relatively high temperatures. Since water solutions were used for spray-drying in the present work, the temperature of the drying gas was set to be 95 °C.

3.2. Phenacetin content in the microparticles.

The average product yield after the spray-drying is 60±5%. The dried samples are white powders. The produced samples were studied with a range of physico-chemical methods.

The phenacetin content in the produced composite was found to be 7.38±0.63% based on the data from UV-spectrophotometry.

3.3. Molecular docking study of PHE-BSA interaction.

Molecular docking study identified 25 binding clusters for domain A and 28 binding clusters in domain B (Fig. 2a, 2b) with a different number of possible conformations. At the same time, PHE-BSA binding energy for the most favorable conformations in each cluster is approximately equal and is in the range between –1.84 kJ/mol and –4.57 kJ/mol.

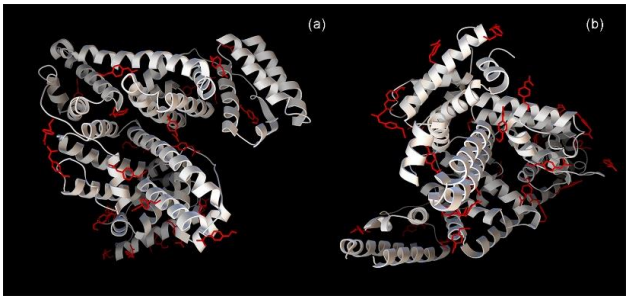

Figure 2. Visualization of molecular docking study of PHE-BSA interaction. Optimal conformations of PHE docked to BSA. a) domain A of BSA, b) domain B of BSA.

The theoretical phenacetin content in the composites, calculated based on the results of the molecular docking study, is 6.85% (the molecular mass of BSA used for calculation is 133423.45 Da according to Brookhaven Protein Data Bank). Experimental content of PHE in microparticles is slightly higher, possibly due to the additional adsorption of PHE molecules on the surface of the protein.

3.4. Residual solvent content.

We have employed TG/DSC analysis to determine a residual solvent content in the microspherical particles. The mass loss of the produced microparticles in the temperature range between 40 and 120 °C is no greater than 4.1% (Fig. 3). This mass loss is accompanied by an endothermal effect in the DSC scan and is related to the loss of the water, which was used as a solvent. Most of the mass loss occurs at temperatures below 100 °C, which indicates an absence of strong intermolecular interactions and may indicate good storage properties even in high humidity conditions.

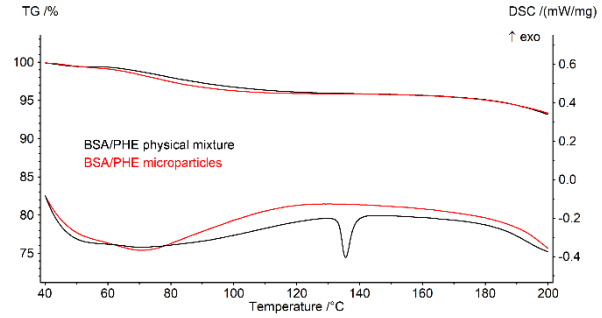

Figure 3. TG/DSC analysis of PHE/BSA physical mixture and microparticles, obtained using spray drying, in the temperature range from 40 to 160 °C in the dynamic argon atmosphere (75 ml/min).

Low residual water content in the produced composites verifies the efficiency of the chosen regime of spray-drying in eliminating the solvent from the resulting microparticles.
Physical mixtures of BSA/PHE with the same PHE content as in microparticles (7.4 %) were produced for comparison. TG curves of microparticles and physical mixtures are virtually the same, which corresponds to the same residual water content in both samples. It is likely that both samples contain the same amount of water corresponding to water molecules occupying hydrophilic centers and reducing the free energy of the system. Such water molecules do not participate in the binding of the drug.
An endotherm of PHE melting is present in the DSC scan of BSA/PHE physical mixture. This effect is not present in the DSC scan of the microparticles. The conventional DSC technique was used for a more detailed investigation of thermal effects.

3.5. Powder X-ray diffractometry results.

Characteristic reflexes of phenacetin are absent from the X-ray powder diffractogram, which indicates a lack of crystalline phase in the produced microparticles and a development of an amorphous PHE phase during spray-drying. Absence of crystal phase of PHE in the produced microparticles may contribute to the enhanced solubility of the drug, as the amorphous phase is more readily soluble than crystalline [37].

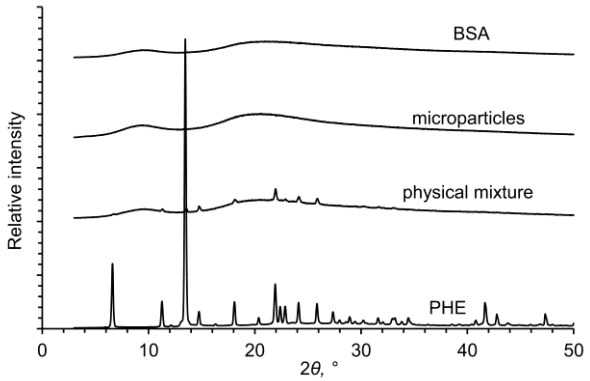

Figure 4. Powder X-ray diffractograms of BSA, PHE, PHE/BSA physical mixture, and microparticles obtained using spray drying.

In the X-ray powder, diffractogram of the PHE/BSA physical mixture with the equivalent content of PHE reflexes of the crystalline phase of the drug is present. Thus, a lack of reflexes of crystal PHE in the diffractograms of the produced microparticles is not caused by a low concentration of the drug but is rather a result of intermolecular interactions between protein and an active ingredient, which prevents the latter from forming a crystalline phase.

3.6. Results of DSC analysis.

Differential scanning calorimetry is more sensitive to the presence of the microcrystalline phase compared to the powder X-ray diffractometry [38]. Thus we have confirmed a lack of crystalline phase of PHE in the microparticles using the DSC technique (Fig 5).

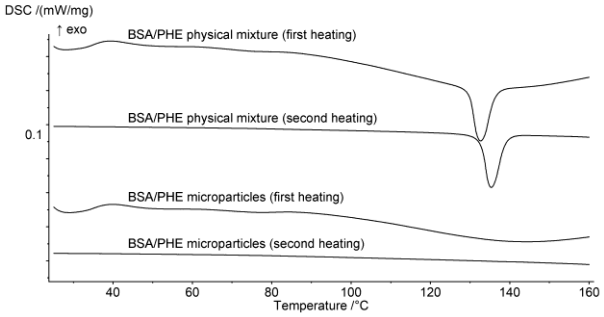

Figure 5. DSC curves of PHE/BSA physical mixture and microparticles obtained using spray drying in the dynamic atmosphere of argon 150 ml/min, temperature range 20–160 °C. First and second heating scans are shown. Heating rate is 5 °C/min.

The absence of endotherm of melting of the drug in the composite is evidence for the lack of crystalline drug in the composite produced by the spray-drying method. At the same time melting endotherm of phenacetin is present in the DSC scans of a physical mixture. Similar results, i.e., a lack of crystalline phase in the microparticles and a presence of the crystalline drug in the physical mixtures were obtained by PXRD method (Fig. 4). Thus, the spray-drying method can be used to produce composites in which the drug included in the protein matrix and is unable to form a crystalline phase.

It should be noted that the fusion enthalpy of phenacetin in the physical mixture (9.3 J/g) is lower than the theoretical value (14.0 J/g) calculated based on the fusion enthalpy of pure phenacetin and its content in the mixture. This fact indicates a partial binding between PHE and BSA developed during the milling process.

Furthermore, fusion enthalpy of phenacetin in the physical mixture, determined during the second heating scan (8.3 J/g) is lower than the fusion enthalpy measured during the first heating scan (9.3 J/g). The decrease in the value of the fusion enthalpy may be caused by the increase of the number of phenacetin molecules bonded to protein, possibly because drug molecules may bind with the centers previously occupied by water molecules. At the same time, the melting temperature of phenacetin in the first scan (132.7 °C) is lower than in the second (135.4 °C) which is likely a result of the growth of the size of phenacetin crystals developed after the first melting.

3.7. FTIR spectroscopy.

The band corresponding to the intermolecular H-bond of the C=O group of phenacetin (νC=O+δCNH 1659 cm^{-1}) is not present in the IR spectra of the BSA/PHE composite microparticles (Fig. 6a, b). This fact indicates a lack of PHE-PHE intermolecular H-bonding in microparticles. At the same time, the bands corresponding to the vibrations of the benzene ring of PHE (δ_{PhH}+ ν_{CC} 1048 cm^{-1}, δ_{PhH}+ δ_{CH3} 1116 cm^{-1}, δ_{PhH} 1174 cm^{-1}, δ_{PhH} + ν_{CN} 1245 cm^{-1}) are visible in the IR spectra [39]. The bands of free and bonded C=O groups of crystalline PHE ($\nu_{C=O}$+δ_{CNH} 1659, 1646 cm^{-1}) are visible in the spectra of the physical mixtures.

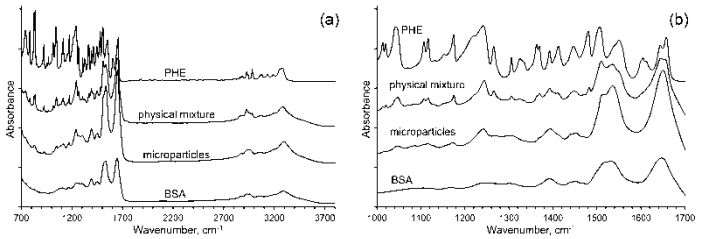

Figure 6. IR spectra of BSA, PHE, microspherical particles formed using spray drying, and PHE/BSA physical mixture in range 700-3800 cm^{-1} (a) and in range 1000-1700 cm^{-1} (b).

It must be noted that the spectra of composites based on BSA are almost identical to that of pure protein which indicates the thermal stability of the protein matrix during the spray drying process.

Thus the data from the IR spectra are in agreement with the data from DSC (Fig. 5) and powder X-ray diffractometry (Fig. 4), which demonstrate a presence of the crystalline phenacetin in the physical mixtures and a lack thereof in the microparticles.

3.8. Scanning electron microscopy data.

The size and morphology of the produced microparticles were studied using scanning electron microscopy; the obtained results are presented in Fig. 7. The peak on the size-distribution curve (Fig. 7c) is rather sharp, which means the produced microparticles are generally uniform in size; the polydispersity index is 0.28. The average particle diameter from the SEM-images is 1.2 μm. The particles have a spherical shape (Fig. 7a), which, together with a lack of agglomeration, should result in favorable aerodynamic characteristics.

The aerodynamic diameter of the produced particles was calculated according to the equation $d_a = d_p\sqrt{\frac{\rho}{1000}}$,

where d_a is aerodynamic diameter, d_p is physical diameter, ρ is the density of the material [40]. The calculated aerodynamic diameter is 1.3 μm, which corresponds to the requirements for the

inhalation delivery systems. The particles of the physical mixture are larger by order of magnitude and have a much more developed surface (Fig. 7b).

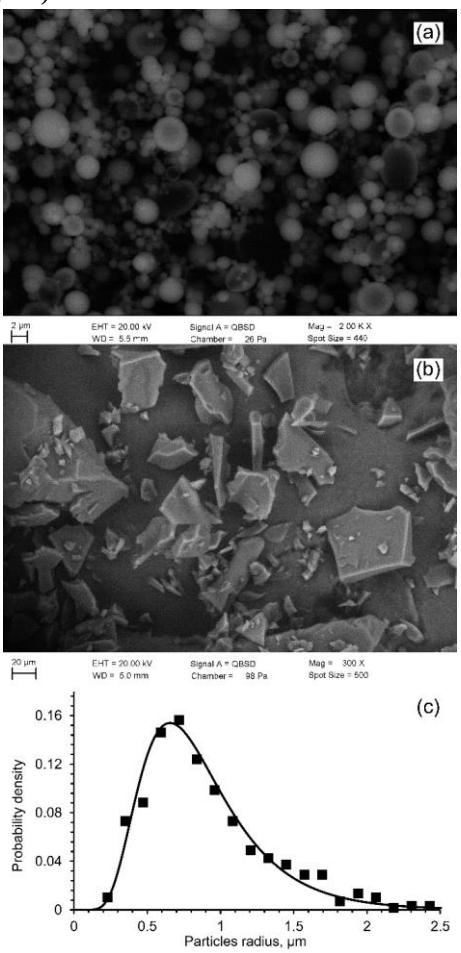

Figure 7. SEM images of PHE/BSA microparticles, obtained using spray drying (a), physical mixture (b), and size distribution curves of microparticles calculated from the image (c).

3.9. Dissolution kinetics. Dissolution kinetics is one of the important factors to be considered for the development of inhalation delivery systems. The dissolution kinetics was studied in the present work at pH 6.86 as the pH of the pleural fluid of the unhealthy patients may drop below 7 [41,42].

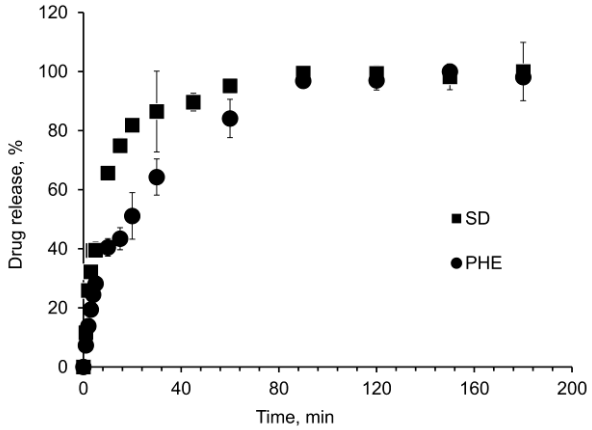

Figure 8. Dissolution profiles of crystalline PHE, microspherical particles of BSA/PHE produced by spray drying in a buffer solution, pH = 6.86 at 37 °C.

The kinetics curves of phenacetin dissolution are demonstrated in Fig.8. As seen from the graph, the rate of release of the drug from the produced microparticles is faster than that of the crystalline phenacetin. For instance, 80% of the drug is released from the microparticles in the first 20 minutes, whereas the release of the same amount of phenacetin into solution from the crystalline drug takes more than an hour. The investigation of the dissolution kinetics demonstrates that the microspherical particles have a high dissolution rate, which allows their use in the inhalation delivery systems for the drugs.

4. CONCLUSIONS

Microspherical particles containing model hydrophobic drug phenacetin were produced using a spray-drying method. The particles were studied with several physicochemical methods, including DSC, SEM, FTIR, and PXRD. It was found that the spray-drying regime used in the present work allows producing microparticles with low residual solvent content. The aerodynamic diameter of the particles is 1.3 μm, which permits their use in inhalation delivery systems.

The dissolution kinetics data demonstrates that the use of the microparticles increases the dissolution rate of phenacetin, which should decrease the time needed to reach a peak concentration of a drug. The results of the present work may be used for the optimization of the process of the production of microparticles of the poorly water-soluble drugs, using the spray-drying method.

5. REFERENCES

1. Loira-Pastoriza, C.; Todoroff, J.; Vanbever, R. Delivery strategies for sustained drug release in the lungs. *Adv. Drug Deliv. Rev.* **2014**, *75*, 81–91, https://doi.org/10.1016/j.addr.2014.05.017.
2. Patton, J.S.; Fishburn, C.S.; Weers, J.G. The lungs as a portal of entry for systemic drug delivery. *Proceedings of the American Thoracic Society* **2004**, *1*, 338–344, https://doi.org/10.1513/pats.200409-049TA.
3. Chen, L.; Okuda, T.; Lu, X.Y.; Chan, H.K. Amorphous powders for inhalation drug delivery. *Adv. Drug Deliv. Rev.* **2016**, *100*, 102–115, https://doi.org/10.1016/j.addr.2016.01.002.
4. Grizić, D.; Lamprecht, A. Microparticle preparation by a propylene carbonate emulsification-extraction method. *Int. J. Pharm.* **2018**, *544*, 213–221. https://doi.org/10.1016/j.ijpharm.2018.03.062
5. Reddy, A.P.; Saheb, S.U.; Maheswari, M.; Suvarsha, G.; Monika, A. Development and evaluation of sustained release microparticles of atenolol of gastrointestinal delivery. *GSCBPS*. **2018**, *03*, 001–005. https://doi.org/10.30574/gscbps.2018.3.2.0026
6. Schulze, J.; Kuhn, S.; Hendrikx, S.; Schulz-Siegmund, M.; Polte, T.; Aigner, A. Spray-Dried Nanoparticle-in-Microparticle Delivery Systems (NiMDS) for Gene Delivery, Comprising Polyethylenimine (PEI)-Based Nanoparticles in a Poly(Vinyl Alcohol) Matrix. *Small.* **2018**, *14*, e1701810, https://doi.org/10.1002/smll.201701810.
7. Olivares, E.C.; Romero, J.L.O.; Méndez, F.B. Microencapsulation of potassium phosphate in chitosan and the effect of spray drying operating variables on the particle size. *J. Mex. Chem. Soc.* **2019**, *62*, 67–74, https://doi.org/10.29356/jmcs.v62i3.452.

8. Benjasirimongkol, P.; Piriyaprasarth, S.; Sriamornsak, P. Improving dissolution and photostability of resveratrol using redispersible dry emulsion: Application of design space for optimizing formulation and spray-drying process. *J. Drug Deliv. Sci. Tec.* **2019**, *51*, 411–418, https://doi.org/10.1016/j.jddst.2019.03.005.
9. Strobel, S.A.; Scher, H.B.; Nitin, N.; Jeoh, T. Control of physicochemical and cargo release properties of cross-linked alginate microcapsules formed by spray-drying. *J. Drug Deliv. Sci. Tec.* **2019**, *49*, 440–447, https://doi.org/10.1016/j.jddst.2018.12.011.
10. Arpagaus, C.; Collenberg, A.; Rütti, D., Assadpour, E.; Jafari, S.M. Nano spray drying for encapsulation of pharmaceuticals. *Int. J. Pharm.* **2018**, *546*, 194–214, https://doi.org/10.1016/j.ijpharm.2018.05.037.
11. Karashima, M.; Sano, N.; Yamamoto, S.; Arai, Y.; Yamamoto, K.; Amano, N.; Ikeda, Y. Enhanced pulmonary absorption of poorly soluble itraconazole by micronized cocrystal dry powder formulations. *Eur. J. Pharm. Biopharm.* **2017**, *115*, 65–72, https://doi.org/10.1016/j.ejpb.2017.02.013.
12. Khadka, P.; Ro, J.; Kim, H.; Kim, I.; Kim, J.T.; Kim, H.; Cho, J.M.; Yun, G.; Lee, J. Pharmaceutical particle technologies: An approach to improve drug solubility, dissolution and bioavailability. *Asian J. Pharm.* **2014**, *9*, 304–316, https://doi.org/10.1016/j.ajps.2014.05.005.
13. Mora-Huertas, C.E.; Fessi, H.; Elaissari, A. Polymer-based nanocapsules for drug delivery. *Int. J. Pharm.* **2010**, *385*, 113–142, https://doi.org/10.1016/j.ijpharm.2009.10.018.
14. Gopi, S.; Amalraj, A.; Thomas, S. Effective drug delivery system of biopolymers based on nanomaterials and hydrogels – a review. *Drug Des.* **2016**, *5*, 1–7, http://dx.doi.org/10.4172/2169-0138.1000129.
15. Tarhinia, M.; Greige-Gerges, H.; Elaissari, A. Protein-based nanoparticles: From preparation to encapsulation of active molecules. *Int. J. Pharm.* **2017**, *522*, 172–197, https://doi.org/10.1016/j.ijpharm.2017.01.067.
16. Liu, Z.; Chen, X. Simple bioconjugate chemistry serves great clinical advances: albumin as a versatile platform for diagnosis and precision therapy. *Chem. Soc. Rev.* **2016**, *45*, 1432–1456, https://doi.org/10.1039/c5cs00158g.
17. Peters, Jr., T. *All About Albumin*. Academic Press: San Diego, USA, 1995; https://doi.org/10.1016/B978-0-12-552110-9.X5000-4.
18. Urien, S.; Tillement, J.P.; Barré, J. The significance of plasma-protein binding in drug research, pharmacokinetic optimization in drug research, In: *Pharmacokinetic Optimization in Drug Research: Biological, Physicochemical and Computational Strategies* Testa, B., van de Waterbeemd, H., Folkers, G., Guy, R. (Eds.), Verlag Helvetica Chimica Acta: Zürich, 2007; pp. 189–197. https://doi.org/10.1002/9783906390437.ch12.
19. Nair, A.B.; Kaushik, A.; Attimarad, M.; Al-Dhubiab, B.E. Enhanced oral bioavailability of calcium using bovine serum albumin microspheres. *Drug Deliv.* **2012**, *19*, 277–285, https://doi.org/10.3109/10717544.2012.704094.
20. Kim, K.J.; Malik, A.B. Protein transport across the lung epithelial barrier. Am. J. Physiol.-Lung Cell. *Mol. Physiol.* **2003**, *284*, L247–L259, https://doi.org/10.1152/ajplung.00235.2002.
21. Elzoghby, A.O.; Samy, W.M.; Elgindy, N.A. Protein-based nanocarriers as promising drug and gene delivery systems. *J. Control. Release.* **2012**, *161*, 38–49, https://doi.org/10.1016/j.jconrel.2012.04.036.
22. Luppi, B.; Cerchiara, T.; Bigucci, F.; Caponio, D.; Zecchi, V. Bovine Serum Albumin Nanospheres Carrying Progesterone Inclusion Complexes. *Drug Deliv.* **2005**, *12*, 281–287, https://doi.org/10.1080/10717540500176704.
23. Salehiabar, M.; Nosrati, H.; Javani, E.; Aliakbarzadeh, F.; Manjili, H.K.; Davaran, S.; Danafar, H. Production of biological nanoparticles from bovine serum albumin as controlled release carrier for curcumin delivery. *Int. J. Biol. Macromol.* **2018**, *115*, 83–89, https://doi.org/10.1016/j.ijbiomac.2018.04.043.
24. Sun, S.; Xiao, Q.R.; Wang, Y.; Jiang, Y. Roles of alcohol desolvating agents on the size control of bovine serum albumin nanoparticles in drug delivery system. *J. Drug Deliv. Sci. Tec.* **2018**, *47*, 193–199, https://doi.org/10.1016/j.jddst.2018.07.018.
25. Casa, D.M.; Scariot, D.B.; Khalil, N.M.; Nakamura, C.V.; Mainardes, R.M. Bovine serum albumin nanoparticles containing amphotericin B were effective in treating murine cutaneous leishmaniasis and reduced the drug toxicity. *Exp. Parasitol.* **2018**, *192*, 12–18, https://doi.org/10.1016/j.exppara.2018.07.003.
26. Wen, Y.; Dong, H.; Li, Y.; Shen, A. Nano-assembly of bovine serum albumin driven by rare-earth-ion (Gd) biomineralization for highly efficient photodynamic therapy and tumor imaging. *J. Mater. Chem. B.* **2016**, *4*, 743–751, https://doi.org/10.1039/c5tb01962a.
27. Fonseca, D.P.; Khalil, N.M.; Mainardes, R.M. Bovine serum albumin-based nanoparticles containing resveratrol: Characterization and antioxidant activity. *J. Drug Deliv. Sci. Tec.* **2017**, *39*, 147–155, https://doi.org/10.1016/j.jddst.2017.03.017.
28. Galukhin, A.; Khelkhal, M.A.; Gerasimov, A.; Biktagirov, T.; Gafurov, M.; Rodionov, A.; Orlinskii, S. Mn-catalyzed oxidation of heavy oil in porous media: Kinetics and some aspects of the mechanism. *Energy Fuels.* **2016**, *30*, 7731–7737, https://doi.org/10.1021/acs.energyfuels.6b01234.
29. Gerasimov, A.V.; Ziganshin, M.A.; Gorbatchuk, V.V. A calorimetric study of the formation of phenacetin solid dispersions with PEG-1400 and pluronic F127. *World Appl. Sci. J.* **2013**, *24*, 920–927.
30. Ziganshin, M.A.; Bikmukhametova, A.A.; Gerasimov, A.V.; Gorbatchuk, V.V.; Ziganshina, S.A.; Bukharaev, A.A. The effect of substrate and air humidity on morphology of films of L-leucyl-L-leucine dipeptide. *Prot. Met. Phys. Chem.* **2014**, *50*, 49–54, https://doi.org/10.1134/S2070205114010171.
31. Ziganshin, M.A.; Gerasimov, A.V.; Ziganshina, S.A.; Gubina, N.S.; Abdullina, G.R.; Klimovitskii, A.E.; Gorbatchuk, V.V.; Bukharaev, A.A. Thermally induced diphenylalanine cyclization in solid phase. *J. Therm. Anal. Calorim.* **2016**, *125*, 905–912, https://doi.org/10.1007/s10973-016-5458-y.
32. Boldyrev, A.E.; Ziganshin, M.A.; Osipov, A.A.; Mukhametzyanov, T.A.; Lyadov, N.M.; Klimovitskii, A.E.; Gerasimov, A.V. Lysozyme-Based Composite Drug Preparations for Inhalation Administration. *BioNanoSci.* **2019**, *9*, 131–140, https://doi.org/10.1007/s12668-018-0576-6.
33. Jarunglumlert, T.; Nakagawa, K. Spray drying of casein aggregates loaded with beta-carotene: Influences of acidic conditions and storage time on surface structure and encapsulation efficiencies. *Dry. Technol.* **2013**, *31*, 1459–1465, https://doi.org/10.1080/07373937.2013.800548.
34. Bhardwaj, U.; Burgess, D.J. A novel USP apparatus 4 based release testing method for dispersed systems. *Int. J. Pharm.* **2010**, *388*, 287–294, https://doi.org/10.1016/j.ijpharm.2010.01.009.
35. Goodsell, D.S.; Morris, G.M.; Olson, A.J. Automated docking of flexible ligands: Application of AutoDock. *J. Mol. Recognit.* **1996**, *9*, 1–5, https://doi.org/10.1002/(SICI)1099-1352(199601)9:1%3C1::AID-JMR241%3E3.0.CO;2-6.
36. Alam, P.; Chaturvedi, S.K.; Anwar, T.; Siddiqi, M.K.; Ajmal, M.R.; Badr, G.; Mahmoud, M.H.; Khan, R.H. Biophysical and molecular docking insight into the interaction of cytosine β-D arabinofuranoside with human serum albumin.

J. Lumin. **2015**, *164*, 123–130, https://doi.org/10.1016/j.jlumin.2015.03.011.
37. Babu, N.J.; Nangia, A. Solubility advantage of amorphous drugs and pharmaceutical Cocrystals. *Cryst. Growth Des.* **2011**, *11*, 2662–2679, https://doi.org/10.1021/cg200492w.
38. Johari, G.P.; Ram, S.; Astl, G.; Mayer, E. Characterizing amorphous and microcrystalline solids by calorimetry. *J. Non-Cryst. Solids.* **1990**, *116*, 282–285, https://doi.org/10.1016/0022-3093(90)90703-O.
39. Burgina, E.B.; Baltakhinov, V.P.; Boldyreva, E.V.; Shakhtschneider, T.P. IR Spectra of Paracetamol and Phenacetin. 1. Theoretical and Experimental Studies. *J Struct. Chem.* **2004**, *45*, 64–73, https://doi.org/10.1023/B:JORY.0000041502.85584.d5.
40. Hinds, W.C. *Aerosol technology: Properties, behavior, and measurement of airborne particles*. John Wiley & Sons: New-York, 1999.
41. Potts, D.E.; Levin, D.C.; Sahn, S.A. Pleural fluid pH in parapneumonic effusions. *Chest*. **1976**, *70*, 328–331, https://doi.org/10.1016/0002-9610(89)90623-5.
42. Houston, M.C. Pleural fluid pH: diagnostic, therapeutic and prognostic value. *Am. J. Surg.* **1987**, *154*, 333–337, https://doi.org/10.1016/0002-9610(89)90623-5.

6. ACKNOWLEDGEMENTS

The reported study was funded by the Russian Foundation for Basic Research according to the research project no. 18-015-00267. N. Lyadov declares that SEM study was performed in the frame of budget plans.